

UC Riverside

UC Riverside Previously Published Works

Title

Tricuspid Valve Regurgitation in Hypoplastic Left Heart Syndrome: Current Insights and Future Perspectives.

Permalink

<https://escholarship.org/uc/item/4117s42q>

Journal

Journal of Cardiovascular Development and Disease, 10(3)

Authors

Ross, Colton
Mir, Arshid
Burkhart, Harold
et al.

Publication Date

2023-03-07



DOI

10.3390/jcdd10030111

Peer reviewed

Review

Tricuspid Valve Regurgitation in Hypoplastic Left Heart Syndrome: Current Insights and Future Perspectives

Colton J. Ross ¹, Arshid Mir ², Harold M. Burkhart ³, Gerhard A. Holzapfel ^{4,5} and Chung-Hao Lee ^{1,*}

¹ Biomechanics and Biomaterials Design Laboratory, University of Oklahoma, Norman, OK 73019, USA

² Department of Pediatrics, University of Oklahoma Health Sciences Center, Oklahoma City, OK 73104, USA

³ Department of Surgery, University of Oklahoma Health Sciences Center, Oklahoma City, OK 73104, USA

⁴ Institute of Biomechanics, Graz University of Technology, 8010 Graz, Austria

⁵ Department of Structural Engineering, Norwegian University of Science and Technology, 7034 Trondheim, Norway

* Correspondence: ch.lee@ou.edu

Abstract: Hypoplastic Left Heart Syndrome (HLHS) is a congenital heart defect that requires a three-stage surgical palliation to create a single ventricle system in the right side of the heart. Of patients undergoing this cardiac palliation series, 25% will develop tricuspid regurgitation (TR), which is associated with an increased mortality risk. Valvular regurgitation in this population has been extensively studied to understand indicators and mechanisms of comorbidity. In this article, we review the current state of research on TR in HLHS, including identified valvular anomalies and geometric properties as the main reasons for the poor prognosis. After this review, we present some suggestions for future TR-related studies to answer the central question: What are the predictors of TR onset during the three palliation stages? These studies involve (i) the use of engineering-based metrics to evaluate valve leaflet strains and predict tissue material properties, (ii) perform multivariate analyses to identify TR predictors, and (iii) develop predictive models, particularly using longitudinally tracked patient cohorts to foretell patient-specific trajectories. Regarded together, these ongoing and future efforts will result in the development of innovative tools that can aid in surgical timing decisions, in prophylactic surgical valve repair, and in the refinement of current intervention techniques.

Keywords: engineering-based analysis; inverse finite element simulations; predictive modeling; surgical intervention; valve tissue biomechanics



Citation: Ross, C.J.; Mir, A.; Burkhart, H.M.; Holzapfel, G.A.; Lee, C.-H. Tricuspid Valve Regurgitation in Hypoplastic Left Heart Syndrome: Current Insights and Future Perspectives. *J. Cardiovasc. Dev. Dis.* **2023**, *10*, 111. <https://doi.org/10.3390/jcdd10030111>

Academic Editors: Lucile Houyel and Damien Bonnet

Received: 14 February 2023

Revised: 24 February 2023

Accepted: 1 March 2023

Published: 7 March 2023



Copyright: © 2023 by the authors. Licensee MDPI, Basel, Switzerland. This article is an open access article distributed under the terms and conditions of the Creative Commons Attribution (CC BY) license (<https://creativecommons.org/licenses/by/4.0/>).

1. Introduction

Hypoplastic Left Heart Syndrome (HLHS) is a congenital heart defect characterized by the underdevelopment of left heart components, including an underdeveloped or undeveloped left ventricle and mitral valve and/or an undersized aorta. Other possible features include a patent ductus arteriosus and a septal–atrial opening, both of which contribute to an oxygenated–deoxygenated blood mixture for systemic perfusion. Regarded together, these key features of HLHS inhibit proper blood flow and require surgical correction almost immediately after birth.

This congenital heart defect has attracted increasing attention over the past two decades (Figure 1) [1–3]. Of those studies, there is a subset of articles dedicated to the understanding of the debilitating comorbidity of tricuspid regurgitation (TR), which is particularly dangerous in this pediatric population. There has also been great progress in distinguishing TR and non-TR cohorts and in determining the risk indicators for TR in HLHS. Looking ahead, it will prove valuable to summarize these works and identify TR indicators that have been unanimously agreed upon, as well as those that are controversial and require further research, and to present studies that will improve our understanding of the tricuspid valve (TV) dysfunction in HLHS.

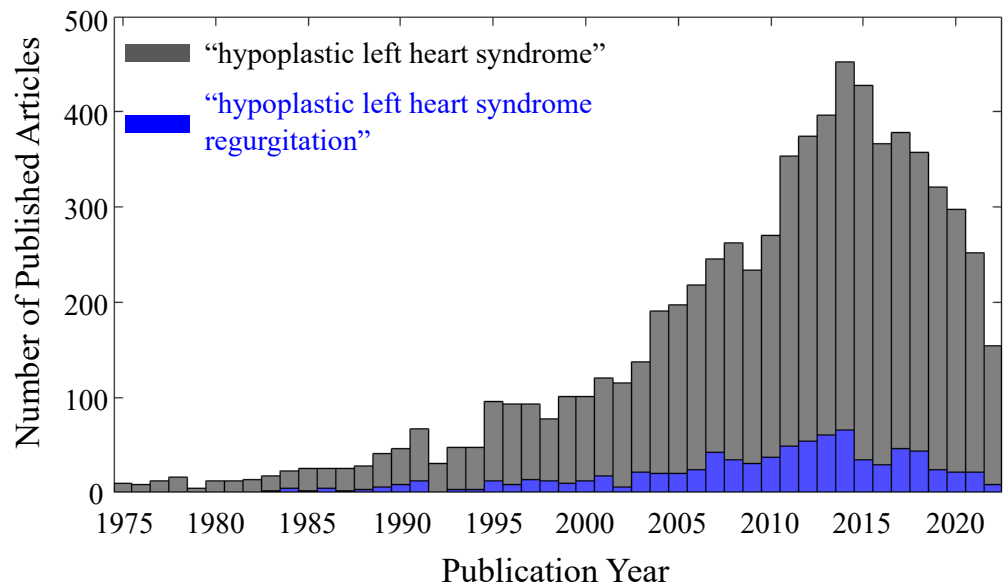


Figure 1. Number of citations per year with the search term ‘hypoplastic left heart syndrome’ (gray bars), superimposed with the subset of citations with the search term ‘hypoplastic left heart syndrome regurgitation’ (blue bars) (data courtesy of Lens).

Current standard practice for the treatment of HLHS, first proposed by Norwood et al. (1980), involves three palliative (i.e., non-curative) cardiac surgeries performed within the first 1.5–3 years of the patient’s life with the overarching goal of creating a functioning single ventricular system (Figure 2) [4,5]. In Stage I Norwood surgery (or Norwood procedure), performed at from 1 to 2 weeks of age, the surgeon establishes an unobstructed blood flow between the right ventricle (RV) and the aorta, enlarges the opening of the atrial septum, and inserts a shunt to the pulmonary artery from either the aorta or the RV [4,6].

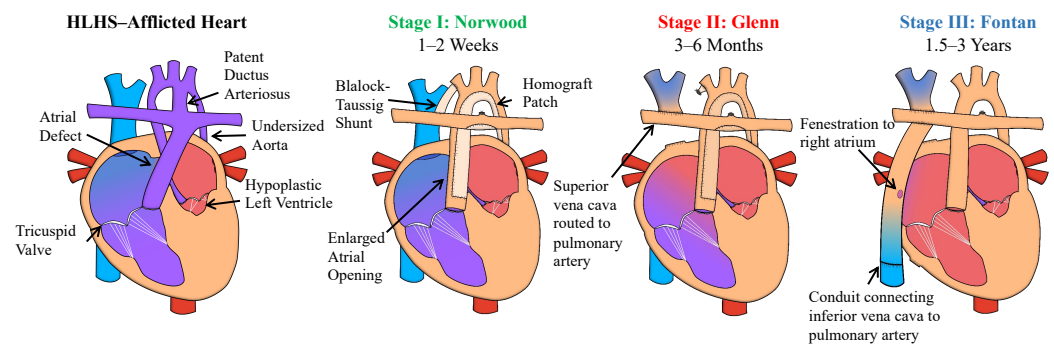


Figure 2. Overview of the characteristics of hypoplastic left heart syndrome (HLHS) and the timeline and surgical corrections for the three-stage cardiac palliative surgeries.

Then, Stage II (i.e., Glenn procedure) is performed at 3–6 months of age, diverting about half of the pulmonary blood flow for passive circulation by rerouting the superior vena cava directly to the pulmonary artery [7,8]. Finally, in Stage III Fontan surgery, performed at 1.5–3 years of age, the surgeon renders the pulmonary blood flow completely passive through a conduit connecting the inferior vena cava to the pulmonary artery, using a fenestration to the right atrium designed to act as a pop-off valve [9,10]. This staged palliation has resulted in a significantly improved mortality, with 87–95% of patients surviving up to 20 years or more after Stage III operation [11–13]. However, TR still represents a challenging risk factor and worsens the quality of life of these infants as they progress into childhood and adulthood.

Specifically, TR is present in up to 25% of all patients with HLHS undergoing staged palliation, which can result in early mortality or require additional risky, invasive TV repair surgeries (e.g., annuloplasty or valvuloplasty) [14–17]. Of the TR-afflicted patients who receive TV repair, from 22 to 48% will need a second TV repair or a total heart transplant within from 5 to 10 years after the first valve repair operation [18–20]. Despite the clear clinical implication of TR in HLHS, to date, there is no consensus on the guidelines or strategies to manage this comorbidity (i.e., valve regurgitation) during the three-stage palliative surgeries, possibly due to limited research to support the creation of such guidelines. Therefore, a special area of research has been devoted to understanding the indicators and mechanisms of TR in newborns with HLHS.

Given the recent advances in HLHS research, our goal in this review article is to provide a concise overview of the risks associated with TR, along with the reported indicators and mechanisms of TR. Additionally, to encourage additional studies in this clinically emerging area, we will recommend some research avenues with a focus on engineering analysis, alternative statistical methods, and predictive modeling that will help improve the current understanding of TR. Future developments such as these will be critical to facilitating personalized risk assessment and refining surgical intervention strategies in HLHS.

2. Tricuspid Regurgitation as a Predictor of Mortality

Historically, there have been mixed results as to whether TR was an indicator of early mortality in HLHS patients. In the period just after the advent of palliative procedure, researchers found that TR was not a significant indicator of early mortality [21–23]. In other studies, TR has even been considered as a contra-indicator for surgical palliation and a predestined early mortality [24–26]. From the perspective of inter-stage periods, Barber et al. (1988) found that TR is a significant survival factor in the inter-Stage I–II period (~35% survival for moderate/severe TR) [14], while other researchers later contradicted this claim and did not believe that inter-stage TR is a significant risk factor [27–30]. The variations in the consideration of TR as a mortality risk extended to the post-Fontan periods.

For example, Chang et al. (1991) found TR to be an indicator for post-palliation mortality [31] and others found that TR did not significantly affect survival [32,33]. The variations in the findings may be explained by a few reasons: (i) some studies were performed shortly after the introduction of the palliative procedure, when early mortality might be due to the surgeon's lack of experience; (ii) in some cases, the statistical analysis may have been biased (e.g., patients organized into groups that could potentially lead to a desired outcome); and (iii) patient selection bias and/or differences in hospital policies may affect study outcomes, such as Mosca et al. (2002) admitting an aggressive policy of performing valvuloplasty for all but mild or traceless TR may have skewed their findings that TR was not a mortality risk [32]. Furthermore, the widespread use of valvuloplasty in Mosca's cohort might indicate that more aggressive treatments do not significantly affect post-Fontan TR-related mortality, and it would be beneficial to confirm this in a future study [32].

In more modern studies, pre-Norwood TR has been clearly associated with increased mortality post-Norwood: an odds ratio (OR) of 2.8 [1.3–6.2] at 95% confidence interval (CI) [34]. The risk of early onset TR was also demonstrated by Sugiura et al. (2014) where they found that patients with TR in the initial palliation stage had a significantly poorer survival time than those who had developed TR in later palliative stages (42.9% vs. 92.9% at 5 years, respectively) [18]. Carlo et al. (2011) came to similar conclusions that the presence of TR on a pre-Glenn echocardiogram was associated with mortality in the interval between Stages II and III (55% attrition rate, together with a hazard ratio (HR) of 6.02 [1.56–23.24] 95% CI); however, the presence of TR in the echocardiogram 'post-Glenn was not recognized as a significant indicator of attrition (27% vs. 5% for with TR and without TR, respectively) [35]. Overall, it is clear that, with continued improvements and surgeons' experience in performing palliative surgery, TR has been considered a significant mortality risk factor, particularly for HLHS patients who develop TR at an earlier age.

Failure of TV Repair and Recurrence of TR

To address TR, TV repair (typically via valvuloplasty [15,32]) is performed either concomitantly with a palliative phase or during the inter-stage period. TV intervention significantly improves the 5-year survival rates (52.1% vs. 23.3% for with and without surgical repair, respectively) [18]. However, 33% of these patients suffer a *recurrent* TR within 5 years of the initial repair [18]. In addition, it was found that the patients who received TV repair concomitant with Stage I (aorta reconstruction) had sub-optimal outcomes at an 8-year follow-up compared to control (non-TR) patients: (i) transplant-free survival rates, 41% and 75% for concomitant TV repair vs. no TR, and (ii) (re-)intervention-free survival rates, 33% and 83% for concomitant TV repair vs. no TR [36]. It is clear that TV interventions for HLHS-afflicted hearts require additional research to improve the intermediate and long-term patient outcomes [37]. As a possibility, an improved understanding of the patient-specific characteristics associated with successful repairs could be beneficial for the refinement of current surgical guidelines. In particular, it was found that successful TV repair associated with the Norwood procedure is related with pre-operative anatomical and functional features: smaller dimensions of the lateral annulus, annular area, and mid-width of the RV, higher anterior leaflet excursion, and presence of anterior leaflet prolapse—the primary TR mechanism as opposed to other causes such as leaflet tethering [36]. Future studies along these lines may reveal further trends in TV apparatus related to desired repair outcomes and lead us to patient-targeted surgical guidelines, such as the suggestion of concomitant vs. inter-stage repair or a specific TV repair technique.

3. Identified Indicators of TR in HLHS

The mortality and risk associated with TR motivates efforts to understand the mechanisms and indicators of comorbidity, which will provide insight to guide and improve the surgical management of HLHS newborns. Additionally, it proves valuable to identify the predictors of TR onset for HLHS patient risk assessment and risk stratification. Here, we summarize some key findings from the recent literature, including geometric differences, structural abnormalities, ventricular mechanics, and surgical decisions that may be associated with TR onset.

3.1. Geometric Differences in TR and Non-TR Cases

Using routine echocardiography and image segmentation techniques, in-depth analyses of valvular geometry have become a promising way to understand the differences between HLHS patients with TR and without TR. For example, Nguyen et al. (2019) analyzed TV geometry in post-Fontan patients and found that patients with TR had a significantly greater change in the annulus area (16.4% vs. 9.3%), circumference (10.5% vs. 4.1%), and in septo-lateral diameter (10.7% vs. 5.7%) during the cardiac cycle compared to those without TR [38]. These changes were also found to vary regionally, with all but the septal annulus quadrant showing significant changes in these geometric quantities. A multivariate logistic regression model also revealed the mid-systolic anterior papillary muscle angle (OR = 2.49[1.34–4.65] 95% CI) and the maximum septo-lateral diameter (OR = 1.73[1.12–2.68] 95% CI) as key metrics related to TR [38]. Future studies conducted in a similar manner will be beneficial to better understand the identified mechanisms of TR identified in previous work, including the structural anomalies (e.g., leaflet tethering or annular dilation), as discussed next.

3.2. Structural Anomalies as Mechanisms of TR

The structural anomalies of the TV are primary contributors to TR in neonates and throughout the palliative series [24]. In the pre-Norwood period, the most common valvular abnormalities associated with TR include annular dilation, leaflet tethering, and chordae shortening [18,36,39–41] (Figure 3). Similar TR mechanisms have been identified in the inter-Stage I–II period along with other additional abnormal features such as leaflet prolapse caused by a flattened annulus and a smaller septal/anterior leaflet area [18,40,42,43]. These findings

were repeated in patients analyzed after post-Glenn, with the primary TR-associated factors found as a dilated annulus (total annular area Z-score, 6.34 ± 2.70 ; lateral dimension Z-score, 4.07 ± 1.70 ; and antero-posterior dimension Z-score, 3.74 ± 1.95), as well as anterior leaflet prolapse [44]. Other investigators also noted a narrowing of the leaflets (OR = 5.8[1.2–28.9] at 95% CI) and annular dilation (OR = 4.1[1.0–16.7] at 95% CI) identified as risk factors for TR after Stage II (the Glenn) palliation [45].

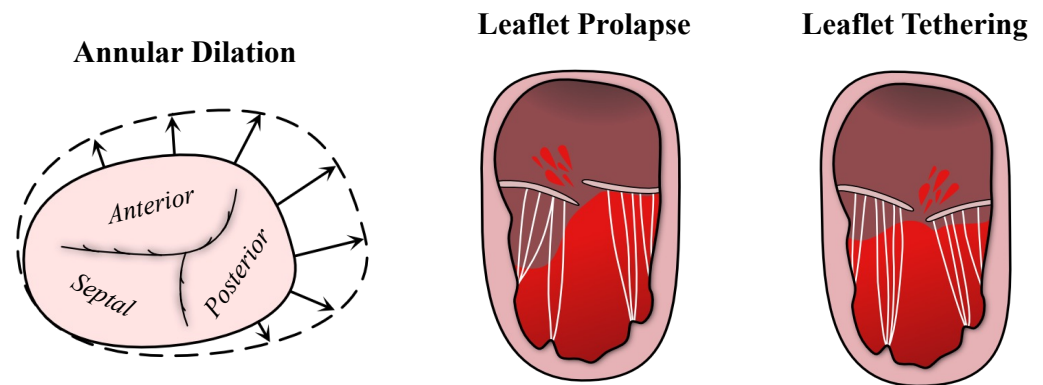


Figure 3. Outlining the predominant mechanisms of tricuspid regurgitation in HLHS.

After the Fontan operation, the patient cohorts were analyzed to determine the from short- to long-term abnormalities associated with TR. Even before Stage I, the metrics were associated with from moderate to severe TR and a lower survival rate post-Fontan: a greater TV tethering volume (0.86 ± 0.60 mL/m² vs. 0.54 ± 0.40 mL/m²: TR vs. non-TR) and annular bending angle ($155.6 \pm 8.9^\circ$ vs. $150.3 \pm 9.2^\circ$: TR vs. non-TR) [41]. The larger tethering volume correlated with the leaflet area (Pearson correlation factor $r = 0.736$), annular area ($r = 0.651$), right ventricular diastolic area ($r = 0.347$), and change in the right ventricular fractional area ($r = -0.387$). In another work, the leaflet tethering was also correlated with right ventricular end-systolic areas ($r = 0.421$), the RV sphericity index ($r = 0.516$), and the angle between the anterior papillary muscle and the ventricular midline ($r = 0.316$) [42]. Similar results were reported by Ono et al. (2020), noting the additional factors attributable to TR: prolapse of the anterior leaflets (52% of patients), restriction of the septal leaflets (50% of patients), annulus dilation (48% of patients), and cleft of the anterior leaflet (21% of patients) [20].

3.2.1. Discrepancy in Findings with a Longitudinal Cohort

The majority of the above studies were conducted without accounting for patient-specific changes in their statistical analysis (i.e., paired samples) that might affect the identified TR-related trends and mechanisms. This is exemplified in the study by Colen et al. (2018), in which they attempted to determine compensatory adaptations of the TV during the pre-Glenn period using a longitudinally tracked cohort [46]. Although they confirmed that TR is associated with larger prolapse volumes and a more flattened and larger annulus, they found that significant TR is associated with *larger* leaflet areas. Interestingly, leaflet coaptation was not significantly different in the TR vs. non-TR groups, and they believe this to be evident for maladaptation of the TV by excessive growth—a theory they have replicated and further explored in a piglet model [42,47]. The inconsistencies in these findings may be due to the improved experimental design, which used measurements from the same patient pre-Norwood and pre-Glenn, in contrast to conflicting data in other works [40]. In the future, prospective studies of this type will provide better insight into the functional changes in TV during palliation periods that can lead to the development, progression, and worsening of TR.

3.2.2. Summary of Primary Structural Findings

Overall, annulus dilation and leaflet prolapse or tethering are unanimously recognized as the primary mechanisms of TR in the HLHS demographic. Furthermore, the geometry of the RV also correlates with the onset of TR—the topic elaborated in Section 3.3. It should also be emphasized that the differences in the results from these studies may be due to the use of unpaired vs. paired statistical analysis designs; additional research may be beneficial to confirm whether tracking patient-specific trajectories is a more accurate method (see Section 4.2.2). In addition, discrepancies between studies may also be due to the limitations of echocardiographic technology, particularly in the previous work, as discussed in the following subsection.

3.2.3. Discrepancies in Echocardiographic Findings

Echocardiographic imaging is a relatively inexpensive, non-invasive (or minimally invasive) imaging modality that is effective in diagnosing valvular disease, but there is a possibility of misdiagnoses. For example, the primary and secondary mechanisms of TR could be misidentified as demonstrated by Bharucha et al. (2013) [45]. In this work, the surgeons identified annular dilation and leaflet dysplasia as the primary TR mechanisms during surgery, while echocardiogram radiologists overwhelmingly reported only leaflet prolapse. Similar discrepancies in echocardiogram-based evaluation and interpretation can be found in the literature describing the location of the regurgitant jet. For example, using 3D echocardiography as a baseline Mah et al. (2021) demonstrated that 2D imaging had lower sensitivity and a poorer accuracy compared to 3D imaging [48]. They observed that, in pre-Glenn patients, the primary jet was in the center of the valve (70% of patients), whereas 2D echo analysis identified the antero-septal commissure as the most common (a finding similar with other 2D imaging work [44]). In a later study analyzing pre- and post-Fontan groups, they found that the center of the valve and the antero-septal commissure were equally common jet locations (45% and 48% of patients, respectively), thus revealing a temporal difference in the jet position [43,48]. Clearly, 3D echocardiography is more recommended for correct valve diagnoses, but the resolution of these images may need to be improved to reduce the inter-study discrepancies. In addition, the guidelines for echocardiogram-based clinical evaluation of TR in HLHS patients could improve diagnostic accuracy, e.g., researchers have advocated detailed temporal analyses of the vena contracta and proximal isovelocity surface measurements to ensure a more accurate and reliable grading of TR severity.

3.3. Ventricular Mechanics and Its Relation to TR

The TV and the RV are structurally and functionally related, and the dysfunction of the RV can also produce an important contribution to the development of TR [49]. From a functional point of view, mechanical dyssynchrony and inhomogeneous contractions of the RV have been identified in the neonatal stage as mechanisms for the occurrence and recurrence of TR [45,50]. At the same time, the presence of TR can impair the RV function, as noted by Bellsham-Revell et al. (2013), who found that the presence of TR increases the indexed end-diastolic volume by 16 mL, on average [51]. RV dysfunction is also influenced by the hypoplastic condition of the left side of the heart, with one study reporting reduced basal-septal RV strains in HLHS patients with a visibly developed left ventricle [52]. There are conflicting reports on whether this hypoplasia is associated with TR: in one study, researchers identified severe underdevelopment of the left-side heart associated with TR in the post-Glenn period [53], while others found this trend in the post-Norwood period [40,52]. From a geometric perspective, greater RV (i.e., apex-to-base length, diastolic area, etc.) was associated with TR throughout the palliative series [18,36,41], i.e., the enlarged RV causes lateral papillary muscle displacement and consequently results in leaflet tethering and TR [39,40]. In conclusion, the function of the RV and TV is clearly closely related, and it is worth exploring RV repair options as a supplement or alternative to traditional TV repairs for HLHS patients undergoing staged palliative surgery.

3.4. Surgical Decisions and Potential Impacts on TR

During palliative procedures, the decisions made during the surgery can affect the development of TR. For example, pre-surgical planning can have a major impact on long-term mortality and outcomes; the type of shunt used in the Norwood procedure can affect TR development; and alternative procedures or modifications of each palliation stage may improve or worsen the patient's subsequent condition. Here, we review the potential impact of these decisions at each stage of the palliation.

3.4.1. Fetal Diagnoses and Pre-Surgical Planning

With recent advances in echocardiographic technology, HLHS and TR can be detected as early as fetal development [54–56]. Prenatal HLHS diagnosis has been associated with a lower incidence of TR [57,58]. However, it is likely that these findings are subject to patient selection bias. Despite this potential limitation, prenatal diagnosis can improve the surgical management of HLHS through prophylactic interventions after birth and pre-planned surgical treatments [57,59], or, in some cases, fetal interventions and HLHS/TR prevention strategies such as balloon dilation [60], maternal hyperoxygenation [61], or aortic valvuloplasty [62]. The preoperative management of HLHS may also affect the development of TR, with one study reporting that neonates without mechanical ventilation were at greater risk of developing TR [63].

3.4.2. Norwood: Shunt Selection

During the Norwood procedure, a shunt is used to increase blood flow to the lungs, and the type of shunt used may vary based on clinician's preference. The two main shunt types seen clinically are the Blalock–Taussig shunt (BTS) and the right ventricle-to-pulmonary artery shunt (RVPAS). The BTS connects the innominate artery or the right subclavian artery (i.e., the first branch of the artery from the aorta) to the pulmonary artery, and Asaki et al. (2014) found that the size of the BTS had a significant impact on the rate of TR prior to the second palliation stage: 3.5 mm shunt, 36% of patients; and 3.0 mm shunt, 7% of patients (OR 7.3[1.4–38] at 95% CI) [64]. Comparing BTS and RVPAS, some researchers have found that RVPAS reduces short-term inter-stage mortality and TR [65], while others found no significant differences in the short-term mortality between the shunt types [66]. However, in the long term, a meta-analysis found that the two shunt types achieved comparable survival in the period between Stages II and III and up to 6 years post-Fontan [67]. This was also evident in a post-Fontan follow-up analysis, although the BTS recipients had higher TR values [68]. Based on these clinical studies, it is possible that there are long-term complications with the RVPAS that cause this ultimate equivalent performance, such as pulmonary artery stenosis and shunt re-interventions. In addition, it is possible that the optimal shunt device or method has yet to be found.

3.4.3. Alternatives to the Norwood Procedure

The hybrid procedure was proposed as an alternative to the Norwood procedure, with the overall goal of avoiding neonatal 'open-heart surgery in infants. In this procedure, a stent is placed via a transcatheter in the patent ductus arteriosus, and the pulmonary arteries are connected in an open-chest procedure to balance the pulmonary and systemic blood flow [69–71]. When comparing the hybrid operation with the traditional Norwood procedure, it was found that the development of the TR does not significantly differ [72,73]. It was also found that the functional indices of RV and TV were not significantly improved in the hybrid procedure and, therefore, the benefits of adopting this hybrid procedure are not clearly demonstrated [73]. Further investigation is needed to determine whether any of the variations of the Norwood procedure (e.g., the Sano modification using the RVPAS) or other alternatives have clear long-term clinical advantages [74].

3.4.4. Stage II (Glenn) Operation

During the Glenn operation, certain surgical decisions may be related to the onset of TR in the pre-Fontan period. For example, it has been observed that recipients of a TV repair at the time of the Glenn surgery have a higher risk of death [75]. Another study also examined the use of a bidirectional superior cavopulmonary anastomosis during the Glenn procedure and found that there was an insignificant difference in the development or severity of occurrence of TR [76]. However, the patients who develop TR after surgery have a higher risk of adverse late effects (OR = 16.5[4.4–62.6] 95% CI) [77]. In some HLHS-specialized centers, the hemi-Fontan procedure is performed instead of the Glenn procedure, facilitating the connection of the superior vena cava to the pulmonary artery with a homograft patch, as opposed to a translocation of the artery to simplify the later Fontan operation [78]. To date, it has been established that the hemi-Fontan procedure is hardly associated with TR [79] and shows similar results to the Glenn in the short-term procedure [80]. Future long-term studies may further demonstrate the benefits or undesirable consequences of these Stage II procedures. For example, it has been theorized that the reduction in the ventricular volume loading after the Glenn procedure may lead to a reduction in TR severity, and, if the appropriate evidence is provided, this information could be useful for determining the surgical timing of Stage II (e.g., performing the operation at an earlier time if the patient has high grade TR) [81].

3.5. Mechanisms of Post-Repair Recurrent TR

In addition to the decisions made during the palliation stages, the method of TV repair can also influence the recurrence of TR. Annuloplasty was predominantly used in one patient cohort and it was found that the repair significantly improved leaflet coaptation lengths, reduced partial change in the RV area and diastolic area, and improved the grade of TR (reduced from 3.1 to 1.7 on a 0.0–4.0 scale) [82]. It has also been shown that preserving RV function in TV repair prevents severe TR recurrence [17,50,83]. It is worth noting that the TV repair can deteriorate the RV function immediately, but long-term improvements are observed such as reduced RV dimensions [15,17,18,82]. In addition, repair beyond an annuloplasty predicts poor prognosis (e.g., mortality) [50]. Other risk factors 5 years after TV repair were analyzed using multivariate analysis: (i) risk factors for mortality—lower weight at time of repair (HR = 0.74[0.55–0.99] 95% CI); (ii) risk factors for re-operation—intervention before Stage II (HR = 5.51[1.063–29.62] 95% CI) and lower weight at initial TV repair (HR = 0.77[0.63–0.95] 95% CI); and (iii) risk factor for TV replacement—pre-Stage II intervention (HR = 36.92[2.17–629.63] 95% CI). Unsuccessful TV repair can also be associated with the presence of posterior leaflet prolapse and septal leaflet tethering [42]. Overall, it is clear that TV repair can be beneficial in preserving RV function and that patients requiring neonatal TV repair typically have poor outcomes. In future studies, analysis of concomitant repair could be beneficial as it is believed that TV intervention prior to RV dysfunction can improve survival in HLHS patients [17,83,84].

4. Lacking Knowledge and Future Perspectives

Although a wide range of research has been conducted to analyze the occurrence or recurrence of TR in HLHS, there are remaining gaps in the knowledge that are critical for refining therapy and assessing patient risk. On the one hand, the list of potential TR indicators may be incomplete, and additional factors need to be considered by analyzing the tissue biomechanics of the TV apparatus. On the other hand, improved statistical designs could provide more accurate predictors of TR and the potential for individualized risk assessment models.

4.1. Engineering Insights for an Improved Understanding of TR

To date, the focus of TR-related research has been on the valvular geometric indicators, structural abnormalities, or problems with TV repair. These findings can also be leveraged by understanding tissue biomechanics, which could provide valuable insights into the

driving mechanisms of TR. For example, excessive tissue strains or stresses, possibly caused by the change in the cardiovascular environment, could indicate the future onset of TR due to deviation from a homeostatic strain or stress that is more desirable for whole valve tissue function and valvular interstitial cells. The development of image-based engineering analysis tools and refined computational models is a crucial next step toward a better understanding of the onset of TR in the HLHS population.

4.1.1. Non-Invasive Analysis of Tissue Biomechanics

Image-based analysis of valvular structures is a research area with growing potential as medical imaging techniques advance. Echocardiograms, in particular, have enabled most of the research examined, and this routine imaging modality can be used for more advanced, engineering-focused analyses. For example, in our research group, we performed image segmentation of the TV annulus in healthy and HLHS-affected newborns to gain preliminary insight into the main differences in valve function: the HLHS-affected TV annulus is larger in circumference, area, and antero-posterior diameter and becomes more circular and curved during valve closure than its healthy counterpart [85]. From an engineering mechanics perspective, the tissue strains did not differ significantly between the cohorts, which may provide an indication that TV is remodeled in the HLHS condition to maintain the homeostatic tissue strain throughout the cardiac cycle [85]. Future research can be performed in a similar way for the TV leaflets to quantify the strains, curvatures, or other biomechanical/geometric factors. In order to enable such an exploration of these dynamic, geometrically complex structures, it can be advantageous to use fully or semi-automated image segmentation methods, such as the recently developed statistical shape modeling technique [86] or deep learning [87,88]. Through the development and refinement of these engineering-focused and automated image segmentation frameworks, the non-invasive analysis of TV becomes more manageable in the clinical setting, which can eventually lead to a detailed, individualized patient risk assessment.

4.1.2. Computational Modeling

Information about tissue strains and geometry can only be obtained using the image-segmented valvular structures, but *in silico* computational modeling, on the other hand, can further predict hemodynamics, tissue material properties, and/or stresses of the TV apparatus *in vivo*. For example, computational models were developed to compare the hemodynamic environment using different shunts in the Norwood procedure [89]. Computational models and simulation frameworks in the HLHS demographic are sparse, and existent modeling techniques for the adult mitral and TV could be adapted for use with the HLHS-afflicted TV to gain new insights into the potential changes in tissue properties that underlie and predict the mechanisms of TR. As an example of how this inverse analysis may be performed, we provide a brief demonstration using our previously presented TV finite element framework [90].

Inverse finite element analysis requires an iterative process to match the ground-truth segmented leaflet surface or point cloud to the finite element mesh. As a proof of concept, we used 3D Slicer (an open-source image segmentation software) to manually trace the TV leaflets of a representative HLHS patient by placing individual points throughout the 3D echocardiogram image stack, obtaining the open (reference configuration) and closed valve geometry (see Figure 4a, and a simplified finite element model in Figure 4b) [91,92]. The open valve geometry was used to generate the finite element mesh for the TV leaflet surface (i.e., a lofted surface, see [93]). Then, the inverse finite element method was applied using the algorithm shown in Figure 4c, where the point cloud from the closed valve state was used to inform the deformed shape of the TV finite element surface. Herein, the residual was defined as the total projected distances of the segmented points to the finite element surface as performed in [94] and a forward difference approximation was used in the gradient-descent optimization algorithm to estimate the material parameters of the functioning TV.

Using this approach, an apparently reasonable match between the point cloud and the finite element surface can be achieved (Figure 4d), and, with refinements, these reconstructions of the TV can become a valuable clinical tool. Specifically, the simulated TV surface can be used for high-resolution visualizations, including more detailed temporal information of the valve closing than can typically be acquired in echocardiography. The predicted tissue properties from the inverse analysis can also be used to perform simulations of different treatment options or disease progression for improved surgical planning. However, it is important to note that the uniqueness of the acquired solution must be guaranteed for accurate predictions of the tissue stresses and material properties, which is a focus of our future research. Another important aspect is the realistic implementation or simplification of the boundary conditions in the simulation, including the transvalvular pressure load and the in vivo motions of the papillary muscle and the TV annulus.

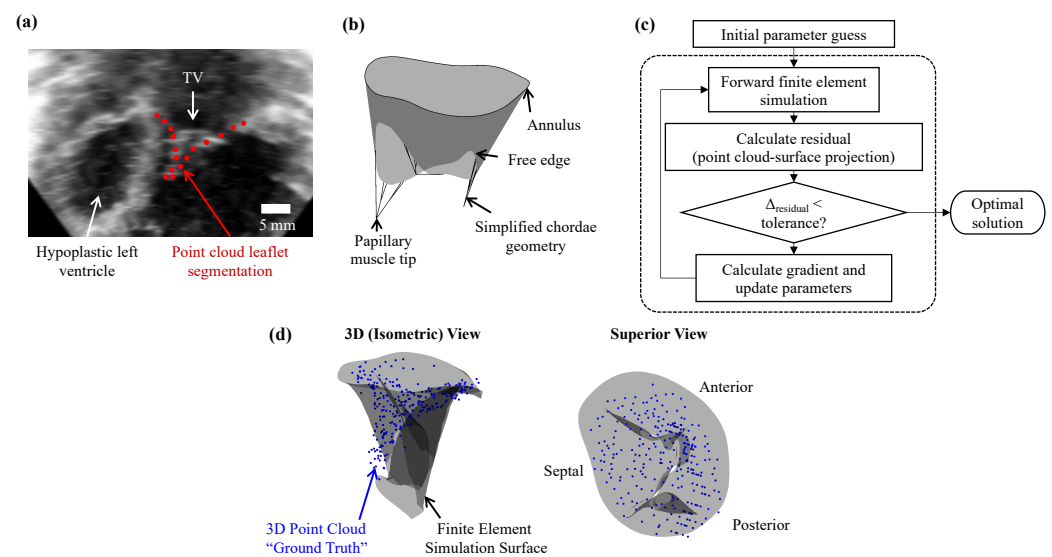


Figure 4. (a) Image segmentation of the TV leaflets from a 3D echocardiogram of a newborn with HLHS; (b) simplified finite element model used in (c) the inverse analysis framework; and (d) representative results from the inverse modeling.

4.2. Statistical Analysis Designs in TR-Related HLHS Research

Most of the work discussed in this article involves analyses of the differences in several recorded measurements and factors between TR and non-TR cohorts relevant to HLHS. Overall, these studies focus on answering the question: *What are the significant differences between HLHS patients with TR and without TR?* While these studies may provide new insights into indicators of TR, a more clinically useful research question exists: *What are the key predictors of TR in the HLHS population during the palliation stages?* To answer this question, another subset of statistical analysis tools must be warranted to obtain the *predictors* of the onset of TR. With more advanced statistical techniques, a predictive model could be developed to determine those patients at risk of TR based on their individual measurements in the clinic. We believe that using multivariate logistic models can lead us to answer the overarching question about the most important TR predictors [95]. To demonstrate the feasibility of this technique, we provide a brief description in the following subsections. In addition to advocating the use of multivariate models, we also briefly discuss the advantages of working with a longitudinally tracked patient cohort, which can more accurately provide the predictors of TR by accounting for patient-specific trajectories.

4.2.1. Demonstration of Multivariate Logistic Modeling

Using our previously presented HLHS patient cohort [85] (IRB #14112 from the University of Oklahoma Health Sciences Center on 12 August 2021), we constructed a *population-averaged* TV geometry as the baseline for elucidating the mechanisms of TR. In short, we first created a

collection of TV geometries covering a range of several key measurements identified as TR indicators in the previous literature: two primary annular diameters, bending angle, three leaflet heights, and area change during TV systolic closure (Table 1, Figure 5a).

Table 1. Range of geometric parameters used to construct the pseudo-population for the multivariate logistic modeling demonstration. Note that the mentioned average values are based on our preliminary observations of a cohort of $n =$ eight neonates born with HLHS.

| Geometry Parameter | Parameter Range | Description |
|----------------------------------|-----------------|--|
| Anterior–Posterior Diameter (mm) | [20.1, 40.2] | 100–200% of the average value for emulating annular dilation |
| Septal–Lateral Diameter (mm) | [16.5, 33.1] | 100–200% of the average value for emulating annular dilation |
| Bending Angle (deg) | [143.5, 175.4] | $\pm 10\%$ of the average value |
| Area Change (%) | [5, 20] | Covering the range described in Section 3.1 |
| Septal Leaflet Height (mm) | [6.6, 19.9] | $\pm 50\%$ of the average value |
| Anterior Leaflet Height (mm) | [7.7, 23.0] | $\pm 50\%$ of the average value |
| Posterior Leaflet Height (mm) | [8.2, 24.5] | $\pm 50\%$ of the average value |

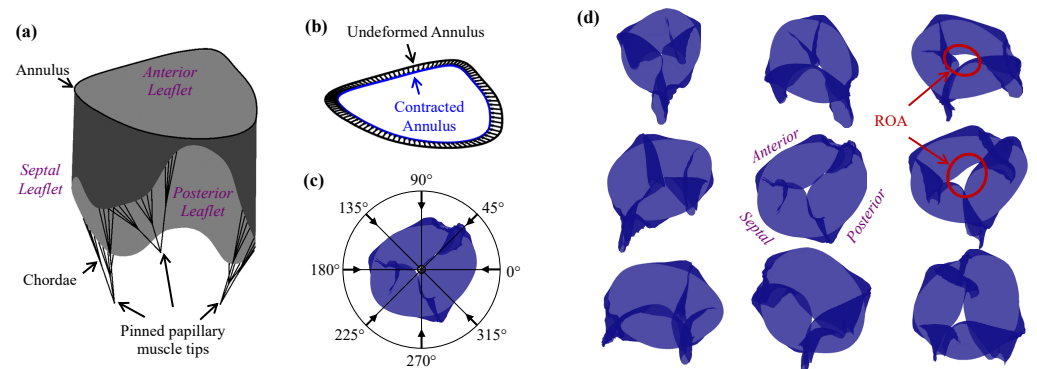


Figure 5. (a) TV model based on the average measurements of our cohort of $n = 8$ neonates with HLHS; (b) visualization of the annulus contraction in the finite element simulations; (c) diagram depicting the top–down viewpoint (represented by the dot) and eight offset viewpoints used to (d) quantify the maximum regurgitation orifice area (all views from the same representative simulation).

These geometries were then used in our finite element simulation framework using the conditions and simulation specifications detailed in [90]. After the finite element simulation was completed, the simulated TV closing surface was exported and post-processed to quantify the regurgitant orifice area (ROA), which represents the TR severity (i.e., the grading of TR). In this procedure, as previously described in [96], the simulated TV surface was projected onto a series of camera viewpoints and the area of the uncoapted region was calculated, using the maximum ROA as a measure of TR severity (Figure 5b). The diagram in Figure 5c shows the top–down viewpoint and the eight offset viewpoints used to quantify the maximum regurgitation orifice area (Figure 5d). To categorize the patients with severe or non-severe TR, we used k -means clustering—an unsupervised classification algorithm (Figure 6a). Here, we briefly highlight that this TR quantification and classification pipeline can be useful in future work with real patient data for automated bulk data processing.

With the binary classification, we then performed a multivariate logistic regression fit using the LASSO algorithm and a 70/30 train/test cross-validation data split [97], with the determined coefficients listed in Table 2. LASSO regression can further be used to find the best n predictors for a multivariate model, which may be useful to determine the trade-off between model simplicity and model accuracy, as visualized by the receiver operating characteristic (ROC) curves (Figure 6b).

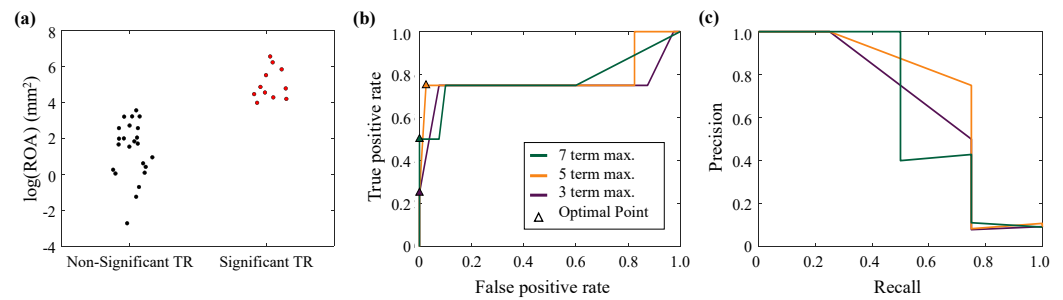


Figure 6. (a) The *k*-means clustering classification of non-TR and TR groups (note that the natural logarithm of the ROA value is used for better visualization); (b) ROC curves generated from multivariate logistic models using a maximum of 3, 5, or 7 predictor variables; and (c) precision–recall curves for each of the multivariate models.

Table 2. Coefficients determined for the multivariate logistic models considering 3, 5, or 7 terms, together with the respective area under the curve to assess the model accuracy. It should be noted that the number of parameters was chosen to obtain unique ROC curves to demonstrate the statistical technique.

| Maximum Number of Parameters | 3 | 5 | 7 |
|----------------------------------|--------|--------|---------|
| Intercept Term | 2.40 | 2.53 | −112.63 |
| Anterior–Posterior Diameter (mm) | 0 | 0.05 | 1.33 |
| Septal–Lateral Diameter (mm) | 0.04 | 0.09 | 1.49 |
| Bending Angle (deg) | 0 | 0 | 0.77 |
| Septal Leaflet Height (mm) | 0 | 0 | 0 |
| Anterior Leaflet Height (mm) | 0 | −0.06 | −1.64 |
| Posterior Leaflet Height(mm) | −0.19 | −0.28 | −3.08 |
| Area Change (%) | −23.06 | −31.48 | −339.19 |
| Area Under the Curve (-) | 0.75 | 0.79 | 0.78 |
| Sensitivity (-) | 0.25 | 0.75 | 0.5 |
| Specificity (-) | 1.00 | 0.98 | 1.00 |

After developing the multivariate model, we also demonstrated the calculation of the key performance metrics, which are crucial for transparency and model assessment. On the one hand, the common performance metrics for predictive models can be summarized into four main categories: (i) *overall performance*, reflecting the differences between the predicted and actual results; (ii) *discrimination*, which describes the effectiveness of the model in distinguishing between events and non-events; (iii) *calibration*, quantifying the agreement between predicted and observed risks; and (iv) *reclassification*, the number of data points that change category with an updated form of the prediction model [98]. On the other hand, the generally adopted assessments for the multivariate logistic models include the *c* statistic (i.e., the area under the ROC curve), sensitivity *SN* (i.e., the true positive rate), specificity *SP*, and the precision *PREC*. The last three metrics can be determined from the number of true positive *TP*, false positive *FP*, false negative *FN*, and true negative *TN* cases based on the optimal threshold value that balances the *TP* and *FP* rates (Figure 5b), i.e.,

$$SN = \frac{TP}{TP + FN}, \quad SP = \frac{TN}{TN + FP}, \quad PREC = \frac{TP}{TP + FP}. \quad (1)$$

For the example models developed in this review, the performance metrics revealed a trade-off between the maximum number of parameters used and the model accuracy, with at least five parameters required for the accurate prediction of the pseudo-patient condition. As an alternate measure of the model performance (particularly in the case of unbalanced observations for each group), the precision–recall (i.e., precision–sensitivity) graph can be used to visualize the model’s ability to discriminate between groups (Figure 6c).

For comparison with the multivariate model, we also performed statistical comparisons of each measurement between the two groups using Student's *t*-test. From this we found significant differences between the two groups for the posterior leaflet height ($p = 0.001$) and the annular area change ($p = 0.001$). Comparing the two statistical modeling approaches, it becomes clear that the metrics that differ significantly from the *t*-tests do not necessarily indicate the measurements needed to accurately predict the onset and development of TR.

In this simple demonstration, we have shown that identifying the *predictors* of TR requires the use of a binary classification technique, such as multivariate logistic regression or support vector machines. By applying the same procedure with real patient data, insights can be obtained to clarify the key indicators of TR. In summary, the multivariate logistic model can be usefully implemented as a supplement to the statistics typically reported in the literature so far and can be helpful to identify the most important TR-related indicators.

4.2.2. Longitudinal Cohorts and Mixed-Effect Models

In a more statistically rigorous study design, longitudinal statistical modeling can provide even better insight into the mechanisms of TR. As a key example of the benefits of conducting a longitudinal study, Colen et al. (2017) found that the leaflet areas *increase* in the presence of TR for their longitudinally tracked, post-Norwood cohort [46], whereas, in another non-paired sample study by Takahashi et al. (2009), TR was associated with *smaller* leaflet areas [40]. By performing a statistical analysis with repeated measurements of the same patient over time, the findings can be more representative of the underlying phenomena in TR due to the complex, multi-factorial nature of this disease condition. Of all the possible methods, mixed-effect models are the primary model of choice for many statisticians for longitudinal predictive modeling, especially on a patient-specific basis [99–101].

In general, mixed-effect models are a class of powerful statistical modeling techniques that incorporate both the population-averaged trends (i.e., fixed-effects) and the patient-specific variations (i.e., mixed effects). In short, these mixed-effect models have the form

$$y_i(t) = \mathbf{b}\mathbf{X} + \mathbf{u}_i\mathbf{Z}_i, \quad (2)$$

where $y_i(t)$ is the outcome of the *i*th patient at time *t*, and \mathbf{b} and \mathbf{u}_i are the coefficients of the fixed-effect parameters \mathbf{X} and the individual-effect parameters \mathbf{Z}_i , respectively, [99,100]. The advantages of this statistical modeling technique include: (i) the model can still be applicable to patient dropout data (e.g., early mortality); (ii) patient-specific predictions can become more dependent on individual trends when each follow-up dataset is considered; and (iii) the time-specific probabilities of TR onset can be determined by implementation with a Cox model. We can therefore use this method in future HLHS research to optimize intervention timing. For example, a prophylactic TV repair concomitant with palliative surgery may be beneficial to proactively correct TR.

5. Conclusions

In this review article, we have provided a summary of the current understanding of the mechanisms and clinical implications of TR in newborns with HLHS. Primarily, TR has been found to be associated with a dilated annulus, leaflet tethering, leaflet prolapse, and right ventricular dysfunction. At the same time, the list of TR identifiers may be incomplete, and future studies focusing on engineering analysis and computational simulations will lay the foundation for a better understanding of the disease state and etiology relevant to the onset and worsening of TR. After this review, we also advocated the use of multivariate logistic models with reports on key performance indicators, which are critical for transparency and possible enrollment in the clinic. Finally, the development of a predictive model could help change the current paradigm for the management of HLHS and patient risk assessment when a longitudinally tracked patient cohort is manageable. Overall, a remarkable amount of work has been performed to understand TR in the HLHS state. Continued efforts to

refine surgical timing and intervention strategies may improve TV repair outcomes and TR-related mortality rates.

Author Contributions: C.J.R. performed the literature review, wrote the first draft of the article, and designed the figures and tables. A.M. and H.M.B. served as clinical consultants to ensure completeness of the review. C.-H.L. and G.A.H. helped to edit and revise the writing. All authors have read and agreed to the published version of the manuscript.

Funding: We acknowledge the supports from the American Heart Association (AHA) Scientist Development Grant Award (16SDG27760143) and the Presbyterian Health Foundation. CJR was in part supported by the National Science Foundation Graduate Research Fellowship (GRF 2020307284). Financial support was provided by the University of Oklahoma Libraries' Open Access Fund.

Institutional Review Board Statement: The study was conducted according to the guidelines of the Declaration of Helsinki, and approved by the Institutional Review Board of University of Oklahoma Health Sciences Center (#14112, 8 December 2021).

Informed Consent Statement: Patient consent was waived because the data were retrospectively collected from the patients.

Data Availability Statement: Not applicable.

Conflicts of Interest: The authors declare no conflict of interest.

References

1. Tchervenkov, C.I.; Jacobs, J.P.; Weinberg, P.M.; Aiello, V.D.; Béland, M.J.; Colan, S.D.; Elliott, M.J.; Franklin, R.C.; Gaynor, J.W.; Krogmann, O.N.; et al. The nomenclature, definition and classification of hypoplastic left heart syndrome. *Cardiol. Young* **2006**, *16*, 339–368. [[CrossRef](#)] [[PubMed](#)]
2. Yabrodi, M.; Mastropietro, C.W. Hypoplastic left heart syndrome: From comfort care to long-term survival. *Pediatr. Res.* **2017**, *81*, 142–149. [[CrossRef](#)] [[PubMed](#)]
3. Saraf, A.; Book, W.M.; Nelson, T.J.; Xu, C. Hypoplastic left heart syndrome: From bedside to bench and back. *J. Mol. Cell. Cardiol.* **2019**, *135*, 109–118. [[CrossRef](#)] [[PubMed](#)]
4. Norwood, W.I.; Kirklin, J.K.; Sanders, S.P. Hypoplastic left heart syndrome: Experience with palliative surgery. *Am. J. Cardiol.* **1980**, *45*, 87–91. [[CrossRef](#)] [[PubMed](#)]
5. Maxwell, J.; Pigott, J.D.; Murphy, J.D.; Barber, G.; Norwood, W.I. Palliative reconstructive surgery for hypoplastic left heart syndrome. *Ann. Thorac. Surg.* **1988**, *45*, 122–128. [[CrossRef](#)]
6. Sano, S.; Ishino, K.; Kawada, M.; Arai, S.; Kasahara, S.; Asai, T.; Masuda, Z.; Takeuchi, M.; Ohtsuki, S. Right ventricle–pulmonary artery shunt in first-stage palliation of hypoplastic left heart syndrome. *J. Thorac. Cardiovasc. Surg.* **2003**, *126*, 504–509. [[CrossRef](#)]
7. Pridjian, A.K.; Mendelsohn, A.M.; Lupinetti, F.M.; Beekman III, R.H.; Dick II, M.; Serwer, G.; Bove, E.L. Usefulness of the bidirectional Glenn procedure as staged reconstruction for the functional single ventricle. *Am. J. Cardiol.* **1993**, *71*, 959–962. [[CrossRef](#)]
8. Scheurer, M.A.; Hill, E.G.; Vasuki, N.; Maurer, S.; Graham, E.M.; Bandisode, V.; Shirali, G.S.; Atz, A.M.; Bradley, S.M. Survival after bidirectional cavopulmonary anastomosis: Analysis of preoperative risk factors. *J. Thorac. Cardiovasc. Surg.* **2007**, *134*, 82–89.e2. [[CrossRef](#)]
9. Fontan, F.; Baudet, E. Surgical repair of tricuspid atresia. *Thorax* **1971**, *26*, 240–248. [[CrossRef](#)]
10. Salazar, J.D.; Zafar, F.; Siddiqui, K.; Coleman, R.D.; Morales, D.L.; Heinle, J.S.; Rossano, J.W.; Mossad, E.B.; Fraser, C.D., Jr. Fenestration during Fontan palliation: Now the exception instead of the rule. *J. Thorac. Cardiovasc. Surg.* **2010**, *140*, 129–136. [[CrossRef](#)]
11. Ono, M.; Boethig, D.; Goerler, H.; Lange, M.; Westhoff-Bleck, M.; Breyman, T. Clinical outcome of patients 20 years after Fontan operation—Effect of fenestration on late morbidity. *Eur. J. Cardio-Thorac. Surg.* **2006**, *30*, 923–929. [[CrossRef](#)] [[PubMed](#)]
12. Pundi, K.N.; Johnson, J.N.; Dearani, J.A.; Pundi, K.N.; Li, Z.; Hinck, C.A.; Dahl, S.H.; Cannon, B.C.; O'Leary, P.W.; Driscoll, D.J.; et al. 40-year follow-up after the Fontan operation: Long-term outcomes of 1052 patients. *J. Am. Coll. Cardiol.* **2015**, *66*, 1700–1710. [[CrossRef](#)] [[PubMed](#)]
13. Poh, C.; d'Udekem, Y. Life after surviving Fontan surgery: A meta-analysis of the incidence and predictors of late death. *Heart Lung Circ.* **2018**, *27*, 552–559. [[CrossRef](#)] [[PubMed](#)]
14. Barber, G.; Helton, J.G.; Aglira, B.A.; Chin, A.J.; Murphy, J.D.; Pigott, J.D.; Norwood, W.I. The significance of tricuspid regurgitation in hypoplastic left-heart syndrome. *Am. Heart J.* **1988**, *116*, 1563–1567. [[CrossRef](#)] [[PubMed](#)]
15. Reyes 2nd, A.; Bove, E.L.; Mosca, R.S.; Kulik, T.J.; Ludomirsky, A. Tricuspid valve repair in children with hypoplastic left heart syndrome during staged surgical reconstruction. *Circulation* **1997**, *96*, II-341–345.
16. Sano, S.; Huang, S.C.; Kasahara, S.; Yoshizumi, K.; Kotani, Y.; Ishino, K. Risk factors for mortality after the Norwood procedure using right ventricle to pulmonary artery shunt. *Ann. Thorac. Surg.* **2009**, *87*, 178–186. [[CrossRef](#)]

17. Elmi, M.; Hickey, E.J.; Williams, W.G.; Van Arsdell, G.; Caldarone, C.A.; McCrindle, B.W. Long-term tricuspid valve function after Norwood operation. *J. Thorac. Cardiovasc. Surg.* **2011**, *142*, 1341–1347. [[CrossRef](#)]
18. Sugiura, J.; Nakano, T.; Oda, S.; Usui, A.; Ueda, Y.; Kado, H. Effects of tricuspid valve surgery on tricuspid regurgitation in patients with hypoplastic left heart syndrome: A non-randomized series comparing surgical and non-surgical cases. *Eur. J. Cardio-Thorac. Surg.* **2014**, *46*, 8–13. [[CrossRef](#)]
19. Alsoufi, B.; Sinha, R.; McCracken, C.; Figueroa, J.; Altin, F.; Kanter, K. Outcomes and risk factors associated with tricuspid valve repair in children with hypoplastic left heart syndrome. *Eur. J. Cardio-Thorac. Surg.* **2018**, *54*, 993–1000. [[CrossRef](#)]
20. Ono, M.; Mayr, B.; Burri, M.; Piber, N.; Röhlig, C.; Strbad, M.; Cleuziou, J.; Hager, A.; Hörer, J.; Lange, R. Tricuspid valve repair in children with hypoplastic left heart syndrome: Impact of timing and mechanism on outcome. *Eur. J. Cardio-Thorac. Surg.* **2020**, *57*, 1083–1090. [[CrossRef](#)]
21. Starnes, V.A.; Griffin, M.L.; Pitlick, P.T.; Bernstein, D.; Baum, D.; Ivens, K.; Shumway, N.E. Current approach to hypoplastic left heart syndrome: Palliation, transplantation, or both? *J. Thorac. Cardiovasc. Surg.* **1992**, *104*, 189–195. [[CrossRef](#)] [[PubMed](#)]
22. Hoshino, K.; Ogawa, K.; Hishitani, T.; Kitazawa, R.; Uehara, R. Hypoplastic left heart syndrome: Duration of survival without surgical intervention. *Am. Heart J.* **1999**, *137*, 535–542. [[CrossRef](#)] [[PubMed](#)]
23. Weinstein, S.; Gaynor, J.W.; Bridges, N.D.; Wernovsky, G.; Montenegro, L.M.; Godinez, R.I.; Spray, T.L. Early survival of infants weighing 2.5 kilograms or less undergoing first-stage reconstruction for hypoplastic left heart syndrome. *Circulation* **1999**, *100*, II167–II170. [[CrossRef](#)]
24. Lang, P.; Norwood, W.I. Hemodynamic assessment after palliative surgery for hypoplastic left heart syndrome. *Circulation* **1983**, *68*, 104–108. [[CrossRef](#)] [[PubMed](#)]
25. Helton, J.; Aglira, B.; Chin, A.; Murphy, J.; Pigott, J.; Norwood, W. Analysis of potential anatomic or physiologic determinants of outcome of palliative surgery for hypoplastic left heart syndrome. *Circulation* **1986**, *74*, 170–176.
26. Hraška, V.; Nosál, M.; Šýkora, P.; Soják, V.; Šagát, M.; Kunovský, P. Results of modified Norwood's operation for hypoplastic left heart syndrome. *Eur. J. Cardio-Thorac. Surg.* **2000**, *18*, 214–219. [[CrossRef](#)]
27. Jonas, R.A.; Hansen, D.D.; Cook, N.; Wessel, D. Anatomic subtype and survival after reconstructive operation for hypoplastic left heart syndrome. *J. Thorac. Cardiovasc. Surg.* **1994**, *107*, 1121–1128. [[CrossRef](#)]
28. Forbess, J.M.; Cook, N.; Roth, S.J.; Serraf, A.; Mayer, J.E., Jr.; Jonas, R.A. Ten-year institutional experience with palliative surgery for hypoplastic left heart syndrome: Risk factors related to stage I mortality. *Circulation* **1995**, *92*, 262–266. [[CrossRef](#)]
29. Hirsch, J.; Ohye, R.; Devaney, E.; Goldberg, C.; Bove, E. The lateral tunnel Fontan procedure for hypoplastic left heart syndrome: Results of 100 consecutive patients. *Pediatr. Cardiol.* **2007**, *28*, 426–432. [[CrossRef](#)]
30. Hehir, D.A.; Dominguez, T.E.; Ballweg, J.A.; Ravishankar, C.; Marino, B.S.; Bird, G.L.; Nicolson, S.C.; Spray, T.L.; Gaynor, J.W.; Tabbutt, S. Risk factors for interstage death after stage 1 reconstruction of hypoplastic left heart syndrome and variants. *J. Thorac. Cardiovasc. Surg.* **2008**, *136*, 94–99.e3. [[CrossRef](#)]
31. Chang, A.C.; Farrell, P.E., Jr.; Murdison, K.A.; Baffa, J.M.; Barber, G.; Norwood, W.I.; Murphy, J.D. Hypoplastic left heart syndrome: Hemodynamic and angiographic assessment after initial reconstructive surgery and relevance to modified Fontan procedure. *J. Am. Coll. Cardiol.* **1991**, *17*, 1143–1149. [[CrossRef](#)]
32. Mosca, R.S.; Kulik, T.J.; Goldberg, C.S.; Vermilion, R.P.; Charpie, J.R.; Crowley, D.C.; Bove, E.L. Early results of the Fontan procedure in one hundred consecutive patients with hypoplastic left heart syndrome. *J. Thorac. Cardiovasc. Surg.* **2000**, *119*, 1110–1118. [[CrossRef](#)]
33. Gaynor, J.W.; Bridges, N.D.; Cohen, M.I.; Mahle, W.T.; DeCampli, W.M.; Steven, J.M.; Nicolson, S.C.; Spray, T.L. Predictors of outcome after the Fontan operation: Is hypoplastic left heart syndrome still a risk factor? *J. Thorac. Cardiovasc. Surg.* **2002**, *123*, 237–245. [[CrossRef](#)] [[PubMed](#)]
34. Shamszad, P.; Gospin, T.A.; Hong, B.J.; McKenzie, E.D.; Petit, C.J. Impact of preoperative risk factors on outcomes after Norwood palliation for hypoplastic left heart syndrome. *J. Thorac. Cardiovasc. Surg.* **2014**, *147*, 897–901. [[CrossRef](#)] [[PubMed](#)]
35. Carlo, W.F.; Carberry, K.E.; Heinle, J.S.; Morales, D.L.; McKenzie, E.D.; Fraser, C.D., Jr.; Nelson, D.P. Interstage attrition between bidirectional Glenn and Fontan palliation in children with hypoplastic left heart syndrome. *J. Thorac. Cardiovasc. Surg.* **2011**, *142*, 511–516. [[CrossRef](#)] [[PubMed](#)]
36. Wamala, I.; Friedman, K.G.; Saeed, M.Y.; Gauvreau, K.; Gellis, L.; Borisuk, M.; Kaza, A.; Emani, S.; Del Nido, P.J.; Baird, C.W. Tricuspid valve repair concomitant with the Norwood operation among babies with hypoplastic left heart syndrome. *Eur. J. Cardio-Thorac. Surg.* **2022**, *62*, ezac033. [[CrossRef](#)]
37. Son, J.S.; James, A.; Fan, C.P.S.; Mertens, L.; McCrindle, B.W.; Manlihot, C.; Friedberg, M.K. Prognostic value of serial echocardiography in hypoplastic left heart syndrome. *Circ. Cardiovasc. Imaging* **2018**, *11*, e006983. [[CrossRef](#)]
38. Nguyen, A.V.; Lasso, A.; Nam, H.H.; Faerber, J.; Aly, A.H.; Pouch, A.M.; Scanlan, A.B.; McGowan, F.X.; Mercer-Rosa, L.; Cohen, M.S.; et al. Dynamic three-dimensional geometry of the tricuspid valve annulus in hypoplastic left heart syndrome with a Fontan circulation. *J. Am. Soc. Echocardiogr.* **2019**, *32*, 655–666. [[CrossRef](#)]
39. Nii, M.; Guerra, V.; Roman, K.S.; Macgowan, C.K.; Smallhorn, J.F. Three-dimensional tricuspid annular function provides insight into the mechanisms of tricuspid valve regurgitation in classic hypoplastic left heart syndrome. *J. Am. Soc. Echocardiogr.* **2006**, *19*, 391–402. [[CrossRef](#)]

40. Takahashi, K.; Inage, A.; Rebeyka, I.; Ross, D.; Thompson, R.; Mackie, A.; Smallhorn, J. Real-time 3-dimensional echocardiography provides new insight into mechanisms of tricuspid valve regurgitation in patients with hypoplastic left heart syndrome. *Circulation* **2009**, *120*, 1091–1098. [[CrossRef](#)]
41. Kutty, S.; Colen, T.; Thompson, R.B.; Tham, E.; Li, L.; Vijarnsorn, C.; Polak, A.; Truong, D.T.; Danford, D.A.; Smallhorn, J.F.; et al. Tricuspid regurgitation in hypoplastic left heart syndrome: Mechanistic insights from 3 to dimensional echocardiography and relationship with outcomes. *Circ. Cardiovasc. Imaging* **2014**, *7*, 765–772. [[CrossRef](#)] [[PubMed](#)]
42. Shigemitsu, S.; Mah, K.; Thompson, R.B.; Grenier, J.; Lin, L.Q.; Silmi, A.; Beigh, M.V.R.; Khoo, N.S.; Colen, T. Tricuspid valve tethering is associated with residual regurgitation after valve repair in hypoplastic left heart syndrome: A three-dimensional echocardiographic study. *J. Am. Soc. Echocardiogr.* **2021**, *34*, 1199–1210. [[CrossRef](#)] [[PubMed](#)]
43. Mah, K.; Khoo, N.S.; Martin, B.J.; Maruyama, M.; Alvarez, S.; Rebeyka, I.M.; Smallhorn, J.; Colen, T. Insights from 3D echocardiography in hypoplastic left heart syndrome patients undergoing TV repair. *Pediatr. Cardiol.* **2022**, *43*, 735–743. [[CrossRef](#)] [[PubMed](#)]
44. Bautista-Hernandez, V.; Brown, D.W.; Loyola, H.; Myers, P.O.; Borisuk, M.; Pedro, J.; Baird, C.W. Mechanisms of tricuspid valve regurgitation in patients with hypoplastic left heart syndrome undergoing tricuspid valvuloplasty. *J. Thorac. Cardiovasc. Surg.* **2014**, *148*, 832–840. [[CrossRef](#)]
45. Bharucha, T.; Honjo, O.; Seller, N.; Atlin, C.; Redington, A.; Caldarone, C.A.; Van Arsdell, G.; Mertens, L. Mechanisms of tricuspid valve regurgitation in hypoplastic left heart syndrome: A case-matched echocardiographic–surgical comparison study. *Eur. Heart J. Cardiovasc. Imaging* **2013**, *14*, 135–141. [[CrossRef](#)]
46. Colen, T.; Kutty, S.; Thompson, R.B.; Tham, E.; Mackie, A.S.; Li, L.; Truong, D.T.; Maruyama, M.; Smallhorn, J.F.; Khoo, N.S. Tricuspid valve adaptation during the first interstage period in hypoplastic left heart syndrome. *J. Am. Soc. Echocardiogr.* **2018**, *31*, 624–633. [[CrossRef](#)]
47. Lin, L.Q.; Hatami, S.; Coe, J.Y.; Colen, T.M.; Sergi, C.; Thompson, R.; Di Martino, E.S.; Herzog, W.; Sara, Z.A.; Freed, D.H.; et al. A novel right ventricular volume and pressure loaded piglet heart model for the study of tricuspid valve function. *J. Vis. Exp.* **2020**, *161*, e61251. [[CrossRef](#)]
48. Mah, K.; Khoo, N.S.; Tham, E.; Yaskina, M.; Maruyama, M.; Martin, B.J.; Alvarez, S.; Alami, N.; Rebeyka, I.M.; Smallhorn, J.; et al. Tricuspid regurgitation in hypoplastic left heart syndrome: Three-dimensional echocardiography provides additional information in describing jet location. *J. Am. Soc. Echocardiogr.* **2021**, *34*, 529–536. [[CrossRef](#)]
49. Ohye, R.G.; Gomez, C.A.; Goldberg, C.S.; Graves, H.L.; Devaney, E.J.; Bove, E.L. Repair of the tricuspid valve in hypoplastic left heart syndrome. *Cardiol. Young* **2006**, *16*, 21–26. [[CrossRef](#)]
50. Ohye, R.G.; Gomez, C.A.; Goldberg, C.S.; Graves, H.L.; Devaney, E.J.; Bove, E.L. Tricuspid valve repair in hypoplastic left heart syndrome. *J. Thorac. Cardiovasc. Surg.* **2004**, *127*, 465–472. [[CrossRef](#)]
51. Bellsham-Revell, H.R.; Tibby, S.M.; Bell, A.J.; Witter, T.; Simpson, J.; Beerbaum, P.; Anderson, D.; Austin, C.B.; Greil, G.F.; Razavi, R. Serial magnetic resonance imaging in hypoplastic left heart syndrome gives valuable insight into ventricular and vascular adaptation. *J. Am. Coll. Cardiol.* **2013**, *61*, 561–570. [[CrossRef](#)] [[PubMed](#)]
52. Forsha, D.; Li, L.; Joseph, N.; Kutty, S.; Friedberg, M.K. Association of left ventricular size with regional right ventricular mechanics in hypoplastic left heart syndrome. *Int. J. Cardiol.* **2020**, *298*, 66–71. [[CrossRef](#)] [[PubMed](#)]
53. Laohachai, K.; Winlaw, D.; Sholler, G.; Veerappan, S.; Cole, A.; Ayer, J. The degree of left ventricular hypoplasia is associated with tricuspid regurgitation severity in infants with hypoplastic left heart syndrome. *Pediatr. Cardiol.* **2019**, *40*, 1035–1040. [[CrossRef](#)] [[PubMed](#)]
54. Muthurangu, V.; Taylor, A.M.; Hegde, S.R.; Johnson, R.; Tulloh, R.; Simpson, J.M.; Qureshi, S.; Rosenthal, E.; Baker, E.; Anderson, D.; et al. Cardiac magnetic resonance imaging after stage I Norwood operation for hypoplastic left heart syndrome. *Circulation* **2005**, *112*, 3256–3263. [[CrossRef](#)]
55. Tongsong, T.; Sittiwangkul, R.; Khunamornpong, S.; Wanapirak, C. Prenatal sonographic features of isolated hypoplastic left heart syndrome. *J. Clin. Ultrasound* **2005**, *33*, 367–371. [[CrossRef](#)]
56. Mart, C.R.; Eckhauser, A.W.; Murri, M.; Su, J.T. A systematic method for using 3D echocardiography to evaluate tricuspid valve insufficiency in hypoplastic left heart syndrome. *Ann. Pediatr. Cardiol.* **2014**, *7*, 193–200. [[CrossRef](#)]
57. Tworetzky, W.; McElhinney, D.B.; Reddy, V.M.; Brook, M.M.; Hanley, F.L.; Silverman, N.H. Improved surgical outcome after fetal diagnosis of hypoplastic left heart syndrome. *Circulation* **2001**, *103*, 1269–1273. [[CrossRef](#)]
58. Kipps, A.K.; Feuille, C.; Azakie, A.; Hoffman, J.I.; Tabbutt, S.; Brook, M.M.; Moon-Grady, A.J. Prenatal diagnosis of hypoplastic left heart syndrome in current era. *Am. J. Cardiol.* **2011**, *108*, 421–427. [[CrossRef](#)]
59. Stoica, S.C.; Philips, A.B.; Egan, M.; Rodeman, R.; Chisolm, J.; Hill, S.; Cheatham, J.P.; Galantowicz, M.E. The retrograde aortic arch in the hybrid approach to hypoplastic left heart syndrome. *Ann. Thorac. Surg.* **2009**, *88*, 1939–1947. [[CrossRef](#)]
60. Tworetzky, W.; Wilkins-Haug, L.; Jennings, R.W.; van der Velde, M.E.; Marshall, A.C.; Marx, G.R.; Colan, S.D.; Benson, C.B.; Lock, J.E.; Perry, S.B. Balloon dilation of severe aortic stenosis in the fetus: Potential for prevention of hypoplastic left heart syndrome: Candidate selection, technique, and results of successful intervention. *Circulation* **2004**, *110*, 2125–2131. [[CrossRef](#)]
61. Szwasz, A.; Tian, Z.; McCann, M.; Donaghue, D.; Rychik, J. Vasoreactive response to maternal hyperoxygenation in the fetus with hypoplastic left heart syndrome. *Circ. Cardiovasc. Imaging* **2010**, *3*, 172–178. [[CrossRef](#)] [[PubMed](#)]

62. Freud, L.R.; McElhinney, D.B.; Marshall, A.C.; Marx, G.R.; Friedman, K.G.; del Nido, P.J.; Emani, S.M.; Lafranchi, T.; Silva, V.; Wilkins-Haug, L.E.; et al. Fetal aortic valvuloplasty for evolving hypoplastic left heart syndrome: Postnatal outcomes of the first 100 patients. *Circulation* **2014**, *130*, 638–645. [[CrossRef](#)] [[PubMed](#)]
63. Sano, S.; Ishino, K.; Kado, H.; Shiokawa, Y.; Sakamoto, K.; Yokota, M.; Kawada, M. Outcome of right ventricle-to-pulmonary artery shunt in first-stage palliation of hypoplastic left heart syndrome: A multi-institutional study. *Ann. Thorac. Surg.* **2004**, *78*, 1951–1958. [[CrossRef](#)] [[PubMed](#)]
64. Asakai, H.; Galati, J.C.; Weskamp, S.; Jones, B.; Millar, J.; Konstantinov, I.E.; d’Udekem, Y.; Brizard, C.P.; Cheung, M.M. Impact of Blalock-Taussig shunt size on tricuspid regurgitation in hypoplastic left heart syndrome. *Ann. Thorac. Surg.* **2014**, *97*, 2123–2128. [[CrossRef](#)] [[PubMed](#)]
65. Pizarro, C.; Mroczek, T.; Malec, E.; Norwood, W.I. Right ventricle to pulmonary artery conduit reduces interim mortality after stage 1 Norwood for hypoplastic left heart syndrome. *Ann. Thorac. Surg.* **2004**, *78*, 1959–1964. [[CrossRef](#)] [[PubMed](#)]
66. Cua, C.L.; Thiagarajan, R.R.; Gauvreau, K.; Lai, L.; Costello, J.M.; Wessel, D.L.; Pedro, J.; Mayer, J.E., Jr.; Newburger, J.W.; Laussen, P.C. Early postoperative outcomes in a series of infants with hypoplastic left heart syndrome undergoing stage I palliation operation with either modified Blalock-Taussig shunt or right ventricle to pulmonary artery conduit. *Pediatr. Crit. Care Med.* **2006**, *7*, 238–244. [[CrossRef](#)]
67. Cao, J.Y.; Phan, K.; Ayer, J.; Celermajer, D.S.; Winlaw, D.S. Long term survival of hypoplastic left heart syndrome infants: Meta-analysis comparing outcomes from the modified Blalock-Taussig shunt and the right ventricle to pulmonary artery shunt. *Int. J. Cardiol.* **2018**, *254*, 107–116. [[CrossRef](#)]
68. Bautista-Hernandez, V.; Scheurer, M.; Thiagarajan, R.; Salvin, J.; Pigula, F.A.; Emani, S.; Fynn-Thompson, F.; Loyola, H.; Schiff, J.; del Nido, P.J.; et al. Right ventricle and tricuspid valve function at midterm after the Fontan operation for hypoplastic left heart syndrome: Impact of shunt type. *Pediatr. Cardiol.* **2011**, *32*, 160–166. [[CrossRef](#)]
69. Galantowicz, M.; Cheatham, J.P. Lessons learned from the development of a new hybrid strategy for the management of hypoplastic left heart syndrome. *Pediatr. Cardiol.* **2005**, *26*, 190–199. [[CrossRef](#)]
70. Lim, D.; Peeler, B.; Matherne, G.; Kron, I.; Gutgesell, H. Risk-stratified approach to hybrid transcatheter-surgical palliation of hypoplastic left heart syndrome. *Pediatr. Cardiol.* **2006**, *27*, 91–95. [[CrossRef](#)]
71. Philip, J.; Reyes, K.; Ebraheem, M.; Gupta, D.; Fudge, J.C.; Bleiweis, M.S. Hybrid procedure with pulsatile ventricular assist device for hypoplastic left heart syndrome awaiting transplantation. *J. Thorac. Cardiovasc. Surg.* **2019**, *158*, e59–e61. [[CrossRef](#)]
72. Chetan, D.; Kotani, Y.; Jacques, F.; Poynter, J.A.; Benson, L.N.; Lee, K.J.; Chaturvedi, R.R.; Friedberg, M.K.; Van Arsdell, G.S.; Caldarone, C.A.; et al. Surgical palliation strategy does not affect interstage ventricular dysfunction or atrioventricular valve regurgitation in children with hypoplastic left heart syndrome and variants. *Circulation* **2013**, *128*, S205–S212. [[CrossRef](#)] [[PubMed](#)]
73. Grotenhuis, H.B.; Ruijsink, B.; Chetan, D.; Dragulescu, A.; Friedberg, M.K.; Kotani, Y.; Caldarone, C.A.; Honjo, O.; Mertens, L.L. Impact of Norwood versus hybrid palliation on cardiac size and function in hypoplastic left heart syndrome. *Heart* **2016**, *102*, 966–974. [[CrossRef](#)] [[PubMed](#)]
74. Fraser, C.D., Jr.; Mee, R.B. Modified Norwood procedure for hypoplastic left heart syndrome. *Ann. Thorac. Surg.* **1995**, *60*, S546–S549. [[CrossRef](#)] [[PubMed](#)]
75. Ashburn, D.A.; McCrindle, B.W.; Tchervenkov, C.I.; Jacobs, M.L.; Lofland, G.K.; Bove, E.L.; Spray, T.L.; Williams, W.G.; Blackstone, E.H.; Society, C.H.S. Outcomes after the Norwood operation in neonates with critical aortic stenosis or aortic valve atresia. *J. Thorac. Cardiovasc. Surg.* **2003**, *125*, 1070–1082. [[CrossRef](#)]
76. Kasnar-Samprec, J.; Kühn, A.; Hörer, J.; Vogt, M.; Cleuziou, J.; Lange, R.; Schreiber, C. Unloading of right ventricle by bidirectional superior cavopulmonary anastomosis in hypoplastic left heart syndrome patients promotes remodeling of systemic right ventricle but does not improve tricuspid regurgitation. *J. Thorac. Cardiovasc. Surg.* **2012**, *144*, 1102–1109. [[CrossRef](#)]
77. Hansen, J.H.; Uebing, A.; Furck, A.K.; Scheewe, J.; Jung, O.; Fischer, G.; Kramer, H.H. Risk factors for adverse outcome after superior cavopulmonary anastomosis for hypoplastic left heart syndrome. *Eur. J. Cardio-Thorac. Surg.* **2011**, *40*, e43–e49. [[CrossRef](#)]
78. Salik, I.; Mehta, B.; Ambati, S. *Bidirectional Glenn Procedure or Hemi-Fontan*; StatPearls Publishing: Tampa, FL, USA, 2020.
79. Douglas, W.I.; Goldberg, C.S.; Mosca, R.S.; Law, I.H.; Bove, E.L. Hemi-Fontan procedure for hypoplastic left heart syndrome: outcome and suitability for Fontan. *Ann. Thorac. Surg.* **1999**, *68*, 1361–1367. [[CrossRef](#)]
80. Edelson, J.B.; Ravishankar, C.; Griffis, H.; Zhang, X.; Faerber, J.; Gardner, M.M.; Naim, M.Y.; Maccio, C.E.; Glatz, A.C.; Goldberg, D.J. A comparison of bidirectional Glenn vs. Hemi-Fontan procedure: An analysis of the single ventricle reconstruction trial public use dataset. *Pediatr. Cardiol.* **2020**, *41*, 1166–1172. [[CrossRef](#)]
81. Alsoufi, B.; Manlhiot, C.; Awan, A.; Alfadley, F.; Al-Ahmadi, M.; Al-Wadei, A.; McCrindle, B.W.; Al-Halees, Z. Current outcomes of the Glenn bidirectional cavopulmonary connection for single ventricle palliation. *Eur. J. Cardio-Thorac. Surg.* **2012**, *42*, 42–49. [[CrossRef](#)]
82. Ugaki, S.; Khoo, N.S.; Ross, D.B.; Rebeyka, I.M.; Adatia, I. Tricuspid valve repair improves early right ventricular and tricuspid valve remodeling in patients with hypoplastic left heart syndrome. *J. Thorac. Cardiovasc. Surg.* **2013**, *145*, 446–450. [[CrossRef](#)] [[PubMed](#)]
83. Bove, E.L.; Ohye, R.G.; Devaney, E.J.; Hirsch, J. Tricuspid valve repair for hypoplastic left heart syndrome and the failing right ventricle. *Semin. Thorac. Cardiovasc. Surg. Pediatr. Card. Surg. Annu.* **2007**, *10*, 101–104. [[CrossRef](#)] [[PubMed](#)]

84. Honjo, O.; Atlin, C.R.; Mertens, L.; Al-Radi, O.O.; Redington, A.N.; Caldarone, C.A.; Van Arsdell, G.S. Atrioventricular valve repair in patients with functional single-ventricle physiology: Impact of ventricular and valve function and morphology on survival and reintervention. *J. Thorac. Cardiovasc. Surg.* **2011**, *142*, 326–335. [[CrossRef](#)] [[PubMed](#)]
85. Ross, C.J.; Trimble, E.J.; Johnson, E.L.; Baumwart, R.; Jolley, M.A.; Mir, A.; Burkhart, H.M.; Lee, C.H. A pilot investigation of the tricuspid valve annulus in newborns with hypoplastic left heart syndrome. *JTCVS Open* **2022**, *10*, 324–339. [[CrossRef](#)]
86. Vicory, J.; Herz, C.; Allemang, D.; Nam, H.H.; Cianciulli, A.; Vigil, C.; Han, Y.; Lasso, A.; Jolley, M.A.; Paniagua, B. Statistical shape analysis of the tricuspid valve in hypoplastic left heart syndrome. In Proceedings of the International Workshop on Statistical Atlases and Computational Models of the Heart, Singapore, 18 September 2021; pp. 132–140. .15. [[CrossRef](#)]
87. Herz, C.; Pace, D.F.; Nam, H.H.; Lasso, A.; Dinh, P.; Flynn, M.; Cianciulli, A.; Golland, P.; Jolley, M.A. Segmentation of tricuspid valve leaflets from transthoracic 3D echocardiograms of children with hypoplastic left heart syndrome using deep learning. *Front. Cardiovasc. Med.* **2021**, *8*, 1839. [[CrossRef](#)]
88. Chen, J.; Li, H.; He, G.; Yao, F.; Lai, L.; Yao, J.; Xie, L. Automatic 3D mitral valve leaflet segmentation and validation of quantitative measurement. *Biomed. Signal Process. Control* **2023**, *79*, 104166. [[CrossRef](#)]
89. Bove, E.L.; Migliavacca, F.; de Leval, M.R.; Balossino, R.; Pennati, G.; Lloyd, T.R.; Khambadkone, S.; Hsia, T.Y.; Dubini, G. Use of mathematic modeling to compare and predict hemodynamic effects of the modified Blalock–Taussig and right ventricle–pulmonary artery shunts for hypoplastic left heart syndrome. *J. Thorac. Cardiovasc. Surg.* **2008**, *136*, 312–320. [[CrossRef](#)]
90. Laurence, D.W.; Johnson, E.L.; Hsu, M.C.; Baumwart, R.; Mir, A.; Burkhart, H.M.; Holzapfel, G.A.; Wu, Y.; Lee, C.H. A pilot in silico modeling-based study of the pathological effects on the biomechanical function of tricuspid valves. *Int. J. Numer. Methods Biomed. Eng.* **2020**, *36*, e3346. [[CrossRef](#)]
91. Lasso, A.; Nam, H.H.; Cianciulli, A.; Pieper, S.; Drouin, S.; Pinter, C.; St-Onge, S.; Vigil, C.; Ching, S.; Sutherland, K.; et al. SlicerHeart: An open-source computing platform for cardiac image analysis and modeling. *Front. Cardiovasc. Med.* **2022**, *9*, 2384. [[CrossRef](#)]
92. Fedorov, A.; Beichel, R.; Kalpathy-Cramer, J.; Finet, J.; Fillion-Robin, J.C.; Pujol, S.; Bauer, C.; Jennings, D.; Fennessy, F.; Sonka, M.; et al. 3D Slicer as an image computing platform for the quantitative imaging network. *Magn. Reson. Imaging* **2012**, *30*, 1323–1341. [[CrossRef](#)]
93. Wu, W.; Ching, S.; Maas, S.A.; Lasso, A.; Sabin, P.; Weiss, J.A.; Jolley, M.A. A computational framework for atrioventricular valve modeling using open-source software. *J. Biomech. Eng.* **2022**, *144*, 101012. [[CrossRef](#)] [[PubMed](#)]
94. Aggarwal, A.; Sacks, M.S. An inverse modeling approach for semilunar heart valve leaflet mechanics: Exploitation of tissue structure. *Biomech. Model. Mechanobiol.* **2016**, *15*, 909–932. [[CrossRef](#)] [[PubMed](#)]
95. Kusiak, A.; Caldarone, C.A.; Kelleher, M.D.; Lamb, F.S.; Persoon, T.J.; Burns, A. Hypoplastic left heart syndrome: Knowledge discovery with a data mining approach. *Comput. Biol. Med.* **2006**, *36*, 21–40. [[CrossRef](#)] [[PubMed](#)]
96. Johnson, E.L.; Laurence, D.W.; Xu, F.; Crisp, C.E.; Mir, A.; Burkhart, H.M.; Lee, C.H.; Hsu, M.C. Parameterization, geometric modeling, and isogeometric analysis of tricuspid valves. *Comput. Methods Appl. Mech. Eng.* **2021**, *384*, 113960. [[CrossRef](#)]
97. Fonti, V.; Belitser, E. Feature selection using LASSO. *VU Amst. Res. Pap. Bus. Anal.* **2017**, *30*, 1–25.
98. Waljee, A.K.; Higgins, P.D.; Singal, A.G. A primer on predictive models. *Clin. Transl. Gastroenterol.* **2014**, *5*, e44. [[CrossRef](#)]
99. Bates, D.; Mächler, M.; Bolker, B.; Walker, S. Fitting linear mixed-effects models using lme4. *J. Stat. Softw.* **2015**, *67*, 1–48. [[CrossRef](#)]
100. Faraway, J.J. *Extending the Linear Model with R: Generalized Linear, Mixed Effects and Nonparametric Regression Models*; Chapman and Hall/CRC: Boca Raton, FL, USA, 2016.
101. Vande Geest, J.P.; Wang, D.H.; Wisniewski, S.R.; Makaroun, M.S.; Vorp, D.A. Towards a noninvasive method for determination of patient-specific wall strength distribution in abdominal aortic aneurysms. *Ann. Biomed. Eng.* **2006**, *34*, 1098–1106. [[CrossRef](#)]

Disclaimer/Publisher’s Note: The statements, opinions and data contained in all publications are solely those of the individual author(s) and contributor(s) and not of MDPI and/or the editor(s). MDPI and/or the editor(s) disclaim responsibility for any injury to people or property resulting from any ideas, methods, instructions or products referred to in the content.